



Cite this: DOI: 10.1039/c8nj03568g

A tripodal supramolecular sensor to successively detect picric acid and CN^- through guest competitive controlled AIE[†]

 Qi Lin,^{ib}*^a Xiao-Wen Guan,^a Yan-Qing Fan,^a Jiao Wang,^a Lu Liu,^a Juan Liu,^b Hong Yao,^{ib}^a You-Ming Zhang^{ib}^a and Tai-Bao Wei^{ib}*^a

Efficient detection of explosives (e.g. picric acid) and toxic compounds (e.g. cyanide) is an important task. Herein, we report a simple and efficient method for the selective and sensitive detection of picric acid (**PA**) and CN^- via a novel guest competitive controlled aggregation-induced emission (AIE) method. First, a tripodal host compound (**TG**) based on a tris-naphthalimide derivative was designed and synthesized. The **TG** can self-assemble to a supramolecular system and show blue AIE. Then, we employed the **TG**-based supramolecular system as a novel supramolecular sensor (**S-TG**). Interestingly, **S-TG** could selectively detect **PA** through a competitive binding interaction, and the detection limit (LOD) of **S-TG** for **PA** is 1.19×10^{-8} M. In this process, the self-assembly of **S-TG** was destroyed and a **TG** and **PA** complex (**TG-PA**) was produced, meanwhile, the AIE of **S-TG** was quenched. More interestingly, **TG-PA** could act as a novel supramolecular sensor for the AIE fluorescent 'turn-on' detection of CN^- , and the LOD of **TG-PA** for CN^- is 7.45×10^{-7} M. Moreover, **PA** and CN^- test kits were prepared by loading **S-TG** or **TG-PA** on silica gel plates. These test kits could conveniently and efficiently detect **PA** or CN^- with high selectivity and sensitivity.

 Received 17th July 2018,
Accepted 5th December 2018

DOI: 10.1039/c8nj03568g

rsc.li/njc

Introduction

The selective and sensitive detection of explosives has attracted increasing attention because it is very important in homeland security and environmental protection.^{1–3} Common explosives are based on nitroaromatic compounds (NACs), such as 2,4,6-trinitrophenol (picric acid (**PA**)), 2,4,6-trinitrotoluene (**TNT**), nitrotoluene (**NT**), 1,3-dinitrobenzene (**DNB**), nitrobenzene (**NB**), etc.⁴ However, among various NACs, **PA** is a widely used explosive because it shows superior explosive power compared to **TNT**.^{5,6} Moreover, **PA** is an important fine chemical and often used in dye industries, pharmaceuticals, and so on.^{7–10} However, because **PA** could cause adverse health effects such as anemia, kidney damage, skin irritation, respiratory system damage and so on,¹¹ **PA** is also considered as a toxic compound

and an environmental pollutant.¹² Simultaneously, due to the high solubility of **PA** in water, it easily contaminates soil and ground water upon exposure. Therefore, the detection of **PA** to avert life safety threats and environmental pollution has been a matter of concern for scientists. To date, many chemosensors such as metal organic frameworks (MOFs),^{13,14} supramolecular organic frameworks (SOFs),¹⁵ polymers,^{16,17} optical sensors,^{18–20} and so on have been reported for the detection of **PA**. Among them, optical sensors are attracting attention for the detection of nitroaromatics owing to their high selectivity and sensitivity, inexpensive nature, rapid response and real-time feasibility in solution.^{21–25} However, although a large number of reports for the detection of nitroaromatics are available,^{26–29} it is still a big challenge to develop effective and easy-to-make chemosensors for convenient detection of **PA**.

In addition, because of the extreme toxicity of cyanide³⁰ and the continuing environmental concern caused by its widespread industrial use,³¹ the highly sensitive and selective detection of cyanide in biological and environmental samples by simple methods has become a very important and challenging task.^{32–34} Many methods, such as electrochemical,³⁵ fluorimetric,³⁶ polarography,³⁷ flow injection amperometric,^{38,39} and chromatographic methods,⁴⁰ have been utilized for the detection of CN^- . However, among these methods, the fluorimetric technique is a highly sensitive, easy, and cheap detection methodology.³⁶

^a Key Laboratory of Eco-Environment-Related Polymer Materials, Ministry of Education of China, Key Laboratory of Polymer Materials of Gansu Province, College of Chemistry and Chemical Engineering, Northwest Normal University, Lanzhou, Gansu, 730070, P. R. China. E-mail: linqi2004@126.com, weitaibao@126.com

^b College of Chemical Engineering, Northwest University for Nationalities, Lanzhou, 730070, China

[†] Electronic supplementary information (ESI) available: Complete experimental procedures and some of the spectroscopic techniques. See DOI: 10.1039/c8nj03568g

Since the concept of aggregation-induced emission (AIE) was proposed by Tang and co-workers in 2001,⁴¹ fluorescent sensors based on AIE fluorophores (AIEgens) have become a hot spot because of their unique photophysical properties.^{42–45} A variety of chemosensors based on AIE fluorophores such as tetraphenylethylene (TPE), silole derivatives, diphenylfumaronitrile derivatives, naphthalimide derivatives, *etc.*, have been reported,⁴⁶ which provide a novel broad platform for the development of AIE-based chemosensors to efficiently detect explosives or toxic compounds. However, to the best of our knowledge, reports on AIE-based chemosensors for effective detection of PA or CN⁻ are very scarce.

In view of this and as part of our research interest in sensors and molecular recognition,^{47–50} herein, we report a simple and efficient method for the selective and sensitive detection of PA and CN⁻ through rationally introducing guest competitive controlled aggregation-induced emission (AIE) into a tris-naphthalimide derivative-based supramolecular sensor. The strategies for the design of the tris-naphthalimide derivative are as follows. First, the naphthalimide moiety acts as the π - π interaction site as well as the fluorescent signal group. Second, an amido group was introduced as the hydrogen bonding site. Fortunately, the tripodal host compound (TG) based on a tris-naphthalimide derivative could self-assemble to a supramolecular system in DMSO solution and shows aggregation-induced emission (AIE). Then, we employed the TG-based supramolecular system as a supramolecular sensor (S-TG). Interestingly, S-TG could selectively detect PA through competitive binding interactions. In this process, the self-assembly of S-TG was destroyed and a TG and PA complex (TG-PA) was produced, meanwhile, the AIE of S-TG was quenched. More interestingly, the complex TG-PA could act as a novel supramolecular sensor for the AIE fluorescent 'turn-on' detection of CN⁻ with high selectivity and sensitivity.

Results and discussion

The novel tripodal compound TG was synthesized by rationally connecting trimesoyl chloride with *N*-(4-(amino)-phenyl)-naphthalimide (DN) through the formation of three amido bonds (Scheme S1, ESI[†]). Interestingly, TG shows blue aggregation-induced emission (AIE) in DMSO solution at $\lambda_{em} = 435$ nm. This fluorescence has been confirmed as AIE through concentration-dependent fluorescence spectroscopy, the Tyndall phenomenon and concentration-dependent ¹H NMR spectroscopy. In the concentration-dependent fluorescence spectra (Fig. S6, ESI[†]), when the TG concentration reached 1×10^{-5} M, the emission intensity at 435 nm showed a sudden increase and the solution emitted blue fluorescence. Meanwhile, as shown in Fig. 1b, TG could dissolve in DMSO and exhibited a clear Tyndall effect. In the concentration-dependent ¹H NMR spectra of TG (Fig. 2), with increasing TG concentration, the signals of the proton H2 on the amido groups exhibited downfield shifts, which indicated that H2 (-NH) formed stable intermolecular hydrogen bonds of -N-H...O=C- with -C=O on adjacent molecules.

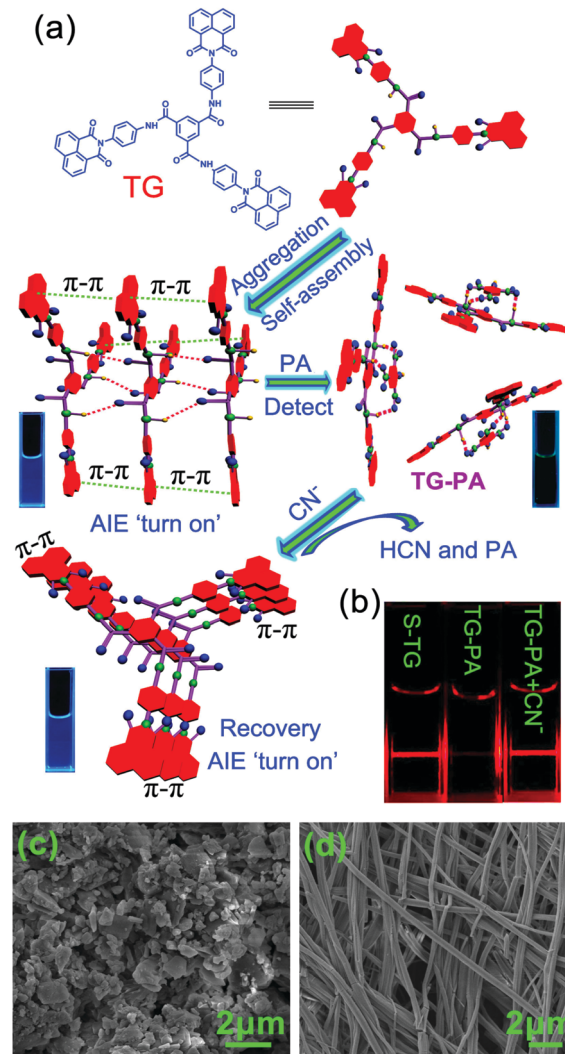


Fig. 1 (a) The structure of TG and the possible recognition mechanism for successively monitoring PA and CN⁻; (b) photo showing the Tyndall effect of S-TG, TG-PA and TG-PA + CN⁻; SEM images of (c) TG and (d) S-TG.

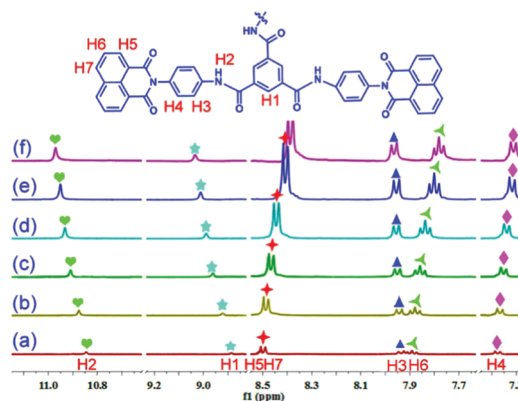


Fig. 2 Partial ¹H NMR spectra of TG in DMSO-*d*₆ at various concentrations: (a) 5.0; (b) 10; (c) 20; (d) 30; (e) 40; (f) 50 mM.

Meanwhile, the signals of the protons H4, H5, H6 and H7 on the naphthalimide group showed obvious upfield shifts,

which suggested that the naphthalimide group was involved in the self-assembly process by π - π stacking interactions.⁵¹ According to the above results, the proposed self-assembly mechanism of **TG** is shown in Fig. 1a; **TG** self-assembled to a supramolecular system (**S-TG**) through π - π and hydrogen bond interactions and showed aggregation-induced emission (AIE). As shown in Fig. 1c and d, using SEM, **TG** exhibits an irregular powder structure (Fig. 1c), while **TG** self-assembled to supramolecular **S-TG** showing graceful uniform fibres (Fig. 1d); this result also showed that **TG** formed the supramolecular polymer **S-TG** by supramolecular interactions.

We employed the **TG**-based supramolecular system as a novel supramolecular sensor, **S-TG**, to detect NACs. The NAC response properties of the sensor **S-TG** were investigated by adding various NACs including picric acid (**PA**), 4-nitroaniline, 4-nitrotoluene, 2,4-dinitrofluorobenzene, 4-nitrochlorobenzene, 2-nitrochlorobenzene, 3-nitrochlorobenzene, 2,4-dinitrochlorobenzene, 3-nitrobromobenzene, 1,3-dinitrobenzene, nitrobenzene, 4-nitroacetophenone, 3-nitrobenzaldehyde, 4-nitrobenzaldehyde, 2-nitrobenzoic acid, 3-nitrobenzoic acid, and 4-nitrobenzoic acid into a DMSO solution of **S-TG** ($c = 1.0 \times 10^{-4}$ M). Interestingly, **S-TG** displayed a very strong emission peak ($\lambda_{em} = 435$ nm) in the corresponding fluorescence spectra. However, after adding 10.0 equivalents of different NACs into the **S-TG** solutions, only **PA** caused the quenching of the fluorescence of **TG** (Fig. 3a and Fig. S7, ESI[†]). Simultaneously, a color change from colorless to yellow was observed by the naked eye upon the addition of **PA** to sensor **S-TG**, in agreement with the appearance of a new absorption band at about 375 nm in the corresponding UV-vis spectrum (Fig. 3b). However, other examined NACs did not cause any similar response. These results suggested that the sensor **S-TG** displayed excellent selectivity to **PA** over all other NACs.

As we all know, selectivity and sensitivity are important features for chemosensors. Therefore, we carefully investigated the specific selectivity of the sensor **S-TG** to **PA** over other miscellaneous competitive NACs by competitive experiments. As shown in Fig. 4, **PA** still produced a similar fluorescence emission response in the presence of other NACs. Moreover, similar competitive experiments were also carried out to study the selective recognition of **S-TG** for **PA** *via* UV-vis spectroscopy (Fig. 5). The results indicated that miscellaneous competitive NACs did not lead to any significant interference in the **PA** sensing process. Therefore, sensor **S-TG** could be used as a fluorescent and colorimetric dual-channel sensor for the detection of **PA**.

In order to evaluate **S-TG** for the detection sensitivity of **PA**, the emission and absorption spectra of sensor **S-TG** were monitored during titration with different concentrations of **PA**. As shown in Fig. S8 (ESI[†]), with increasing amounts of **PA**, a gradual decrease in the emission intensity of **S-TG** at 435 nm was observed. Simultaneously, as shown in Fig. S9 (ESI[†]), approximately 99.2% fluorescence emission quenching was observed upon the addition of 10.0 equivalents of **PA**. Correspondingly, in the absorption spectra (Fig. S10, ESI[†]), upon successive addition of 0–14 equivalents of **PA** to a DMSO solution of **S-TG**, a new absorption peak at 375 nm gradually increased.

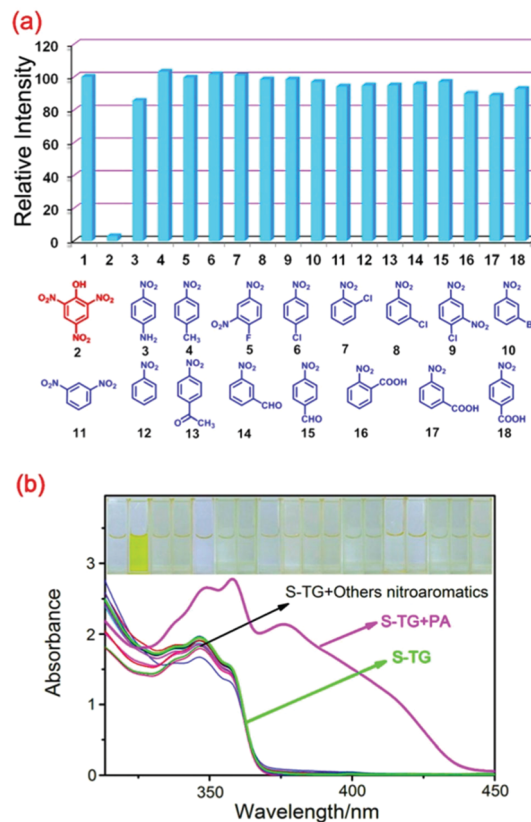


Fig. 3 (a) Fluorescence emission of the **S-TG** (1.0×10^{-4} M) in the presence of different nitroaromatics (0.01 M); (b) absorbance spectra of the **S-TG** (1.0×10^{-4} M) in the presence of different nitroaromatics (0.01 M) in DMSO solution.

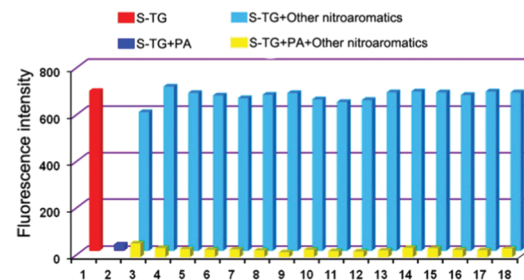


Fig. 4 Fluorescence intensity response of the **S-TG** (1.0×10^{-4} M) and **PA** (10 equiv.) in the presence of various nitroaromatics in DMSO solution.

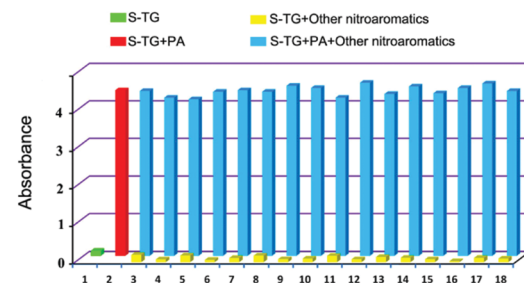


Fig. 5 Absorption intensity response of **S-TG** (1.0×10^{-4} M) and **PA** (10 equiv.) in the presence of various nitroaromatics in DMSO solution.

Finally, the detection limit of **S-TG** for **PA** determined by the emission and absorption spectroscopy titrations and calculated on the basis of the $3\sigma/s$ method⁵² was 1.19×10^{-8} M and 1.38×10^{-8} M, respectively (Fig. S11 and S12, ESI†).

Moreover, the fluorescence emission response of **S-TG** to **PA** was analyzed by the linear part of the Stern–Volmer equation:¹⁹ $I_0/I = 1 + K_{SV}[Q]$, where I_0 is the initial fluorescence intensity of **TG** before the addition of **PA**, I is the fluorescence intensity after the addition of **PA**, $[Q]$ is the molar concentration of **PA**, and K_{SV} is the quenching constant (M^{-1}). The Stern–Volmer plots for **PA** are nearly linear at low concentrations ($R^2 = 0.99405$) and the constant K_{SV} for **PA** was found to be $7.40 \times 10^4 M^{-1}$ (Fig. 6). In addition, a comprehensive comparison of **TG** with some reported materials for the detection for **PA** is listed in Table S1 (ESI†), which indicated that **S-TG** has a more sensitive response ability to **PA** than most reported sensors.

The recognition mechanism of **S-TG** for **PA** was carefully investigated *via* 1H NMR, FT-IR and ESI-MS spectroscopies. In the 1H NMR titration experiments (Fig. S13, ESI†), with the addition of different equivalents of **PA** into a DMSO- d_6 solution of **TG** (1.0×10^{-4} M), all of the aromatic protons (H3–H7) on **TG** showed downfield shifts, which indicated that the π - π interactions in the self-assembled supramolecular system of **S-TG** were destroyed. Meanwhile, the signals of H2 on the amido group of **TG** and Hp on **PA** showed distinct downfield shifts, which indicated that H2 formed stable intermolecular hydrogen bonds with $-NO_2$ on **PA** molecules. Meanwhile, in the corresponding IR spectra (Fig. S14, ESI†), the $-NH$ and $=C-H$ stretching vibration absorption peaks of **TG** appeared at 3423 and 2928 cm^{-1} respectively; however, in a mixture of **TG** and **PA**, the $-NH$ and $=C-H$ stretching vibration absorption peaks shifted to 3415 and 2920 cm^{-1} , which indicated that **TG** and **PA** formed stable intermolecular hydrogen bonds through the $-NH$ on the amido groups of **TG** and $-NO_2$ on **PA** (Fig. 1a). These results suggested that the addition of **PA** destroyed the self-assembly of **S-TG**, which induced quenching of the AIE of **S-TG**, meanwhile, a novel host-guest complex **TG-PA** was formed. The proposed mechanism was confirmed by the ESI-MS spectra (Fig. S15, ESI†); when excess **PA** was added to a solution of **TG**, a peak for $[TG + PA + Na^+]$ (m/z 1272.2407) was found at 1272.2116, indicating the formation of the stabilized host-guest complex **TG-PA** (1 : 1 stoichiometry).

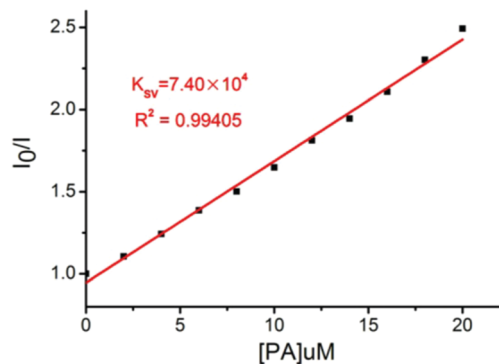


Fig. 6 Stern–Volmer plot for **PA** at a lower concentration.

Interestingly, the complex **TG-PA** could be employed as a novel supramolecular sensor for the fluorescent “turn-on” detection of CN^- . The anion response properties of **TG-PA** were carefully investigated by adding various water solutions of anions (AcO^- , $H_2PO_4^-$, HSO_4^- , ClO_4^- , F^- , Cl^- , Br^- , I^- , SCN^- and CN^-) into the DMSO solution of **TG-PA** ($c = 1.0 \times 10^{-4}$ M). **TG-PA** exhibits negligible fluorescence emission, while with the gradual addition of CN^- , the **TG-PA** solution shows a gradual increase of the emission intensity at 450 nm (Fig. 7a). Meanwhile, a bright blue fluorescence could be distinguished by the naked eye under a UV-lamp (365 nm) as shown in Fig. 7a. In comparison, the addition of various other anions such as AcO^- , $H_2PO_4^-$, HSO_4^- , ClO_4^- , F^- , Cl^- , Br^- , I^- and SCN^- to the solution of **TG-PA** showed very slight changes. These results clearly suggested that sensor **TG-PA** exhibited high selectivity to CN^- over other anions.

Then, competitive experiments were carried out by adding 60.0 equiv. of a CN^- water solution and 60.0 equiv. of various anion water solutions to the **TG-PA** DMSO solution ($c = 1.0 \times 10^{-4}$ M). The fluorescence selectivity was examined at an emission wavelength of 450 nm in the presence of other anions, and showed that all the competing anions did not interfere in the detection of CN^- (Fig. 7b). This result showed the high selectivity of the sensor **TG-PA** toward CN^- over the other analytes mentioned above.

To further investigate the efficiency of sensor **TG-PA** toward CN^- detection, we carried out fluorescence titration experiments.

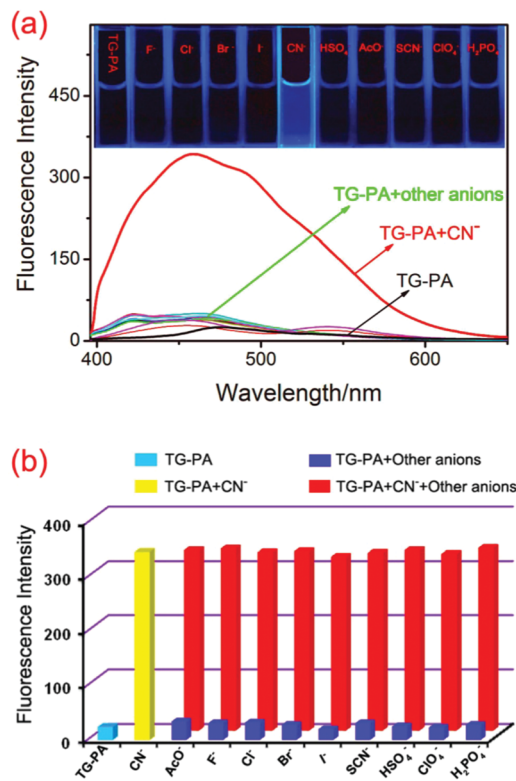


Fig. 7 (a) Fluorescence spectra of **TG-PA** (1.0×10^{-4} M) in DMSO in the presence of various anions; (b) fluorescence intensity response of **TG-PA** (1.0×10^{-4} M) and CN^- in the presence of various anions in DMSO solution.

As shown in the fluorescence spectrum, addition of increasing amounts of CN^- ions to the solution of **TG-PA** directly leads to the emission 'turn-on' (Fig. S16, ESI[†]). Strikingly, an excellent linear dependence ($R^2 = 0.98902$) of the concentration of CN^- was observed. Meanwhile, the detection limit of the fluorescence titration spectrum changes calculated on the basis of the $3\sigma/s$ method⁵² is 7.45×10^{-7} M (Fig. S17, ESI[†]), indicating the high sensitivity of the sensor to CN^- .

The recognition mechanism of **TG-PA** for CN^- was carefully investigated *via* ^1H NMR and IR spectroscopies. As shown in the ^1H NMR spectra (Fig. 8), with increasing CN^- concentrations, the signals of the H2 on the amido groups of **TG** gradually disappeared; this result indicated that CN^- caused the H2 to undergo a deprotonation process, which broke the intermolecular hydrogen bonding between **TG** and **PA** and caused the destruction of the sensor **TG-PA** complex (Fig. 1). Meanwhile, Hp on **PA** showed upfield shifts because of the shielding effect. Simultaneously, the H4, H5, H6 and H7 protons showed slight upfield shifts, which indicated that **TG** recovered its self-assembly by π - π interactions, meanwhile, the AIE of **S-TG** was recovered (Fig. 1). To further understand the process, FT-IR spectroscopy of **TG** was carried out (Fig. S14, ESI[†]); the $-\text{NH}$ and $=\text{C}-\text{H}$ stretching vibration absorption peaks of **TG-PA** appeared at 3415 and 2920 cm^{-1} , respectively, when CN^- was added to a solution of the **TG-PA** complex, and the stretching vibration absorption peaks of $-\text{NH}$ disappeared, meanwhile the $=\text{C}-\text{H}$ absorption peaks shifted to 2930 cm^{-1} . These results also support the above-mentioned proposed mechanism.

In order to investigate the application of sensor **S-TG** for the convenient detection of **PA**, a **PA** test kit was prepared by loading **S-TG** on a silica gel plate. The test kit exhibits a bright blue fluorescence emission. As shown in Fig. 9a, upon the addition of a solution of **PA**, we found that the silica gel plate-based **PA** test kit showed distinct fluorescence quenching. The results indicated that the detection limit of **PA** was 1.0×10^{-8} M. Therefore, the **S-TG**-based silica gel plates could act as a novel and efficient test kit for convenient detection of **PA** in solution. Meanwhile, in the corresponding solid state emission

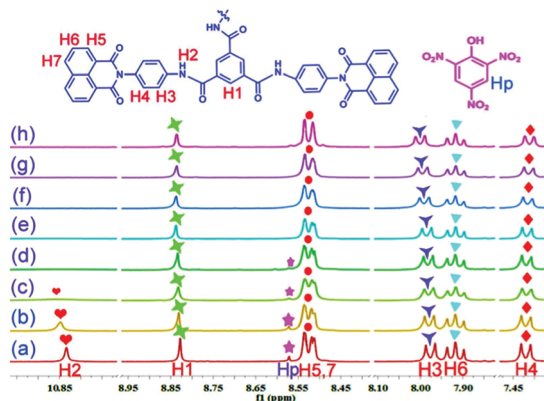


Fig. 8 Partial ^1H NMR spectra of **TG** and **PA** (1:1) in $\text{DMSO}-d_6$ with different equivalents of CN^- : (a) 0; (b) 0.2; (c) 0.4; (d) 0.6; (e) 0.8; (f) 1.0; (g) 2.0; (h) 3.0.

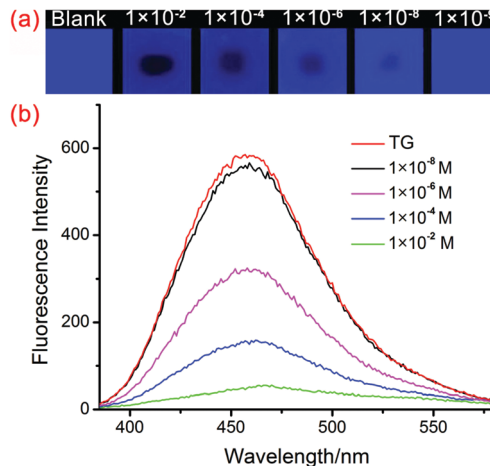


Fig. 9 (a) Photographs of the paper test strips of probe **TG** under UV light (365 nm) and (b) solid state emission spectra of **TG** with the addition of different concentrations of **PA**.

spectra (Fig. 9b), along with the increasing amounts of **PA**, the emission intensity of **TG** showed a gradual decrease.

Subsequently, to investigate the practical applications of **TG-PA**, CN^- test kits were prepared by loading **TG-PA** on silica gel plates. Test kits containing **TG-PA** were utilized to detect CN^- . As shown in Fig. S18 (ESI[†]), when CN^- water solution was added to the test kits, a fluorescence turn on response can be observed under a 365 nm UV-lamp. In order to investigate the practical applications of the sensor **TG-PA** for the detection of CN^- , we employed peach seeds as a practical sample.³² The experiments were carried out as follows: 50 grams of peach seeds was crushed and pulverized, and then, 200 mL of water was added to the pulverized peach seeds, and the resulting turbid solution was vigorously stirred for 30 min. After this,

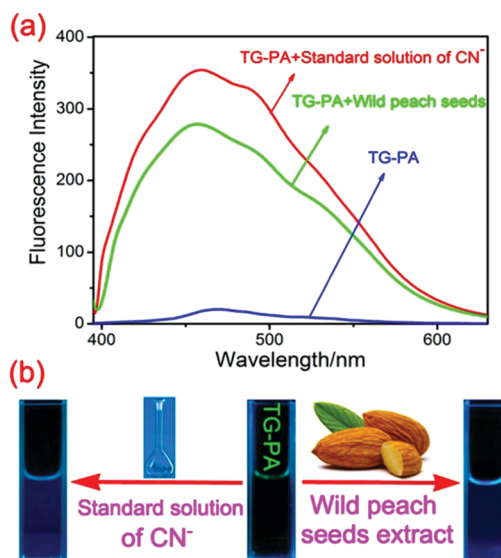


Fig. 10 (a) Fluorescence spectra of **TG-PA** (1.0×10^{-4} M) in the presence of two different cyanide solutions in DMSO ($\lambda_{\text{ex}} = 370$ nm); (b) response photographs of **TG-PA** in wild peach seeds and standard solution of CN^- .

the turbid solution was filtered and a practical sample solution was obtained. As shown in Fig. 10a, upon the addition of the practical sample solution into **TG-PA** (1.0×10^{-4} M), the fluorescence intensity of sensor **TG-PA** increased rapidly. The bright blue fluorescence could be distinguished by the naked eye under a UV lamp (365 nm), as shown in Fig. 10b. These results indicated that sensor **TG-PA** could efficiently detect CN^- through fluorescent “turn-on” in a practical sample.

Conclusions

In summary, a tripodal host compound **TG** based on a trisnaphthalimide derivative was designed and synthesized. The **TG** could self-assemble to a supramolecular system (**S-TG**) and show aggregation-induced emission (AIE). Interestingly, **S-TG** could selectively and sensitively detect picric acid (**PA**). Moreover, **TG** could form a stable **TG-PA** complex and act as a novel supramolecular sensor for the fluorescence “turn-on” detection of CN^- . The recognition mechanism of **S-TG** for **PA** and **TG-PA** for CN^- is based on a novel guest competitive controlled aggregation-induced emission (AIE) process. Meanwhile, test kits based on **S-TG** and **TG-PA** for convenient fluorescence detection of **PA** and CN^- were prepared. Moreover, **TG-PA** can detect CN^- through fluorescence in a practical sample. It is worth mentioning that the novel recognition mechanism based on the guest competitive controlled aggregation-induced emission (AIE) process provides a new way for the design of fluorescent sensors.

Conflicts of interest

There are no conflicts to declare.

Acknowledgements

This work was supported by the National Natural Science Foundation of China (NSFC) (No. 21574104; 21662031; and 21661028) and the Program for Changjiang Scholars and Innovative Research Team in the University of Ministry of Education of China (IRT 15R56).

Notes and references

- L. L. Zhang, Z. X. Kang, X. L. Xin and D. F. Sun, *CrystEngComm*, 2016, **18**, 193.
- W. Wang, J. Yang, R. M. Wang, L. L. Zhang, J. F. Yu and D. F. Sun, *Cryst. Growth Des.*, 2015, **15**, 2589.
- Y. Salinas, R. M. Martinez, M. D. Marcos, F. Sancenon, A. M. Costero, M. Parra and S. Gil, *Chem. Soc. Rev.*, 2012, **41**, 1261.
- M. E. Germain and M. J. Knapp, *Chem. Soc. Rev.*, 2009, **38**, 2543.
- B. O. Okesola and D. K. Smith, *Chem. Soc. Rev.*, 2016, **45**, 4226.
- Y. Yao, M. Xue, J. Chen, M. Zhang and F. Huang, *J. Am. Chem. Soc.*, 2012, **134**, 15712.
- S. S. Nagarkar, B. Joarder, A. K. Chaudhari, S. Mukherjee and S. K. Ghosh, *Angew. Chem., Int. Ed.*, 2013, **52**, 2881.
- J. Shen, J. Zhang, Y. Zuo, L. Wang, X. Sun, J. Li, W. Han and R. He, *J. Hazard. Mater.*, 2009, **163**, 1199.
- Y. Ma, S. Huang, M. Deng and L. Wang, *ACS Appl. Mater. Interfaces*, 2014, **6**, 7790.
- A. Ding, L. M. Yang, Y. Y. Zhang, G. B. Zhang, L. Kong, X. J. Zhang, Y. P. Tian, X. T. Tao and J. X. Yang, *Chem. – Eur. J.*, 2014, **20**, 12215.
- K. M. Wollin and H. H. Dieter, *Arch. Environ. Contam. Toxicol.*, 2005, **49**, 18.
- G. He, H. Peng, T. Liu, M. Yang, Y. Zhang and Y. Fang, *J. Mater. Chem.*, 2009, **19**, 7347.
- X. Z. Song, S. Y. Song, S. N. Zhao, Z. M. Hao, M. Zhu, X. Meng, L.-L. Wu and H.-J. Zhang, *Adv. Funct. Mater.*, 2014, **24**, 4034.
- Y. Takashima, V. M. Martinez, S. Furukawa, M. Kondo, S. Shimomura, H. Uehara, M. Nakahama, K. Sugimoto and S. Kitagawa, *Nat. Commun.*, 2011, **2**, 168.
- Y. Zhang, T. G. Zhan, T. Y. Zhou, Q. Y. Qi, X. N. Xu and X. Zhao, *Chem. Commun.*, 2016, **52**, 7588.
- A. S. G. Liu, D. Luo, N. Li, W. Zhang, J. L. Lei, N. B. Li and H. Q. Luo, *ACS Appl. Mater. Interfaces*, 2016, **8**, 21700.
- S. Shanmugaraju, C. Dabadie, K. Byrne, A. J. Savyasachi, D. Umadevi, W. Schmitt, J. A. Kitchen and T. Gunnlaugsson, *Chem. Sci.*, 2017, **8**, 1535.
- V. Bhalla, A. Gupta and M. Kumar, *Org. Lett.*, 2012, **14**, 3112.
- M. C. Rong, L. P. Lin, X. H. Song, T. T. Zhao, Y. X. Zhong, J. W. Yan, Y. R. Wang and X. Chen, *Anal. Chem.*, 2015, **87**, 1288.
- B. Gogoi and N. S. Sarma, *ACS Appl. Mater. Interfaces*, 2015, **7**, 11195.
- S. Hussain, A. H. Malik, M. A. Afroz and P. K. Iyer, *Chem. Commun.*, 2015, **51**, 7207.
- V. Bereau, C. Duhayon and J. P. Sutter, *Chem. Commun.*, 2014, **50**, 12061.
- D. Dinda, A. Gupta, B. K. Shaw, S. Sadhu and S. K. Saha, *ACS Appl. Mater. Interfaces*, 2014, **6**, 10722.
- K. K. Kartha, S. S. Babu, S. Srinivasan and A. Ajayaghosh, *J. Am. Chem. Soc.*, 2012, **134**, 4834.
- S. S. Nagarkar, B. Joarder, A. K. Chaudhari, S. Mukherjee and S. K. Ghosh, *Angew. Chem., Int. Ed.*, 2013, **52**, 2881.
- J. Ma, T. Lin, X. Pan and W. Wang, *Chem. Mater.*, 2014, **26**, 4221.
- H. T. Feng and Y. S. Zheng, *Chem. – Eur. J.*, 2014, **20**, 195.
- N. Dey, S. K. Samanta and S. Bhattacharya, *ACS Appl. Mater. Interfaces*, 2013, **5**, 8394.
- K. Dhanunjayarao, V. Mukundam and K. Venkatasubbaiah, *Inorg. Chem.*, 2016, **55**, 11153.
- Z. C. Xu, X. Q. Chen, H. N. Kim and J. Y. Yoon, *Chem. Soc. Rev.*, 2010, **39**, 127.
- S. Vallejos, P. Estevez, F. C. Garcia, F. Serna, J. L. de la Pena and J. M. Garcia, *Chem. Commun.*, 2010, **46**, 7951.
- W. J. Qu, W. T. Li, H. L. Zhang, T. B. Wei, Q. Lin, H. Yao and Y. M. Zhang, *Sens. Actuators, B*, 2017, **241**, 430.

- 33 F. Wang, L. Wang, X. Chen and J. Yoon, *Chem. Soc. Rev.*, 2014, **43**, 4312.
- 34 D. G. Cho and J. L. Sessler, *Chem. Soc. Rev.*, 2009, **38**, 1647.
- 35 M. A. Kaloo and J. Sankar, *Chem. Commun.*, 2015, **51**, 14528.
- 36 M. Shamsipur and H. R. Rajabi, *Mater. Sci. Eng., C*, 2014, **36**, 139.
- 37 D. Bohrer, C. P. Nascimento, S. Garcia Pomblum, E. Seibert and L. M. D. Carvalho, *Anal. Chem.*, 1998, **361**, 780.
- 38 H. Sulistyarti and S. D. Kolev, *Microchem. J.*, 2013, **111**, 103.
- 39 S. Dadfarnia, M. A. H. Shabani, F. Tamadon and M. Rezaei, *Microchim. Acta*, 2007, **158**, 159.
- 40 B. Desharnais, G. Huppe, M. Lamarche, P. Mireault and C. D. Skinner, *Forensic Sci. Int.*, 2012, **222**, 346.
- 41 J. Luo, Z. Xie, J. W. Y. Lam, L. Cheng, H. Chen, C. Qiu, H. S. Kwok, X. Zhan, Y. Liu, D. Zhu and B. Z. Tang, *Chem. Commun.*, 2001, 1740.
- 42 X. Li, M. Jiang, J. W. Y. Lam, B. Z. Tang and J. Y. Qu, *J. Am. Chem. Soc.*, 2017, **139**, 17022.
- 43 P. Zhang, Z. Zhao, C. Li, H. Su, Y. Wu, R. T. K. Kwok, J. W. Y. Lam, P. Gong, L. Cai and B. Z. Tang, *Anal. Chem.*, 2018, **90**, 1063.
- 44 Y. Hong, J. W. Y. Lam and B. Z. Tang, *Chem. Soc. Rev.*, 2011, **40**, 5361.
- 45 T. Jiang, H. Q. Tan, Yi. Sun, J. Wang, Y. D. Hang, N. Lu, J. Yang, X. Qu and J. L. Hua, *Sens. Actuators, B*, 2018, **261**, 115.
- 46 D. Ding, K. Li, B. Liu and B. Z. Tang, *Acc. Chem. Res.*, 2013, **46**, 2441.
- 47 Q. Lin, T. T. Lu, X. Zhu, T. B. Wei, H. Li and Y. M. Zhang, *Chem. Sci.*, 2016, **7**, 5341.
- 48 Q. Lin, Y. Q. Fan, P. P. Mao, L. Liu, J. Liu, Y. M. Zhang, H. Yao and T. B. Wei, *Chem. – Eur. J.*, 2018, **24**, 777.
- 49 Q. Lin, K. P. Zhong, J. H. Zhu, L. Ding, J. X. Su, H. Yao, T. B. Wei and Y. M. Zhang, *Macromolecules*, 2017, **50**, 7863.
- 50 J. F. Chen, Q. Lin, Y. M. Zhang, H. Yao and T. B. Wei, *Chem. Commun.*, 2017, **53**, 13296.
- 51 S. S. Babu, V. K. Praveen and A. Ajayaghosh, *Chem. Rev.*, 2014, **114**, 1973.
- 52 Analytical Methods Committee, *Analyst*, 1987, **112**, 199.